computational models

Causes of spherical aberration induced by laser refractive surgery

Geunyoung Yoon, PhD, Scott MacRae, MD, David R. Williams, PhD, Ian G. Cox, PhD

Purpose: To develop a corneal model to better explain how refractive surgery procedures induce spherical aberration.

Setting: Department of Ophthalmology and Center for Visual Science, University of Rochester, Rochester, New York, USA.

Methods: The preoperative cornea was modeled as a rotationally symmetric surface with various radii of curvature and asphericities. The postoperative cornea was defined as the difference between the preoperative cornea and an ablation thickness profile computed based on the Munnerlyn equation. A ray-tracing program and Zernike polynomial fitting were used to calculate the induced amount of spherical aberration assuming a fixed ablation depth per pulse or a variable ablation depth depending on the incidence angle of each pulse on the cornea. A biological eye model of the corneal surface change after laser refractive surgery was also developed to explain the induced spherical aberrations after myopic and hyperopic treatments.

Results: The clinical data showed that positive spherical aberration was induced after myopic correction and negative spherical aberration increased after hyperopic correction. In contrast, assuming a fixed ablation depth per pulse, the theoretical prediction was that negative spherical aberration with myopic treatment and positive spherical aberration with hyperopic treatment would increase. However, when assuming a variable ablation depth per pulse caused by non-normal incidence of laser spot on the cornea, the theoretically predicted induction of spherical aberration tends to fit better with the myopic and hyperopic clinical data. The effect of a variable ablation depth accounted for approximately half the clinically observed amount of spherical aberration. The biological model of the corneal surface change used to explain this remaining discrepancy showed the magnitude of the biological response in myopic correction is 3 times smaller than in hyperopic correction and that the direction of the biological response in hyperopic treatment is opposite that in myopic treatment.

Conclusions: This nontoric eye model, which separates the effects of differences in ablation efficiency and biological corneal surface change quantitatively, explains how spherical aberration is induced after myopic and hyperopic laser refractive surgery. With the corneal topographic data, this model can be incorporated into the ablation algorithm to decrease induced spherical aberrations, improving the outcomes of conventional and customized treatments.

J Cataract Refract Surg 2005; 31:127–135 © 2005 ASCRS and ESCRS

Wavefront-sensing techniques provide a precise understanding of the optical quality of the eye before and after laser refractive surgery and assist in further refinements of ablation algorithms to enhance the predictability of surgical outcomes. These techniques also make it possible to correct higher-order aberrations (HOAs) using advanced methods such as adaptive optics, customized laser refractive surgery, and customized optics. Even though conventional and customized laser refractive surgery techniques have proved

effective in improving patient visual performance, a better understanding of the wave aberration induced by a laser ablation procedure is required to achieve greater improvement in vision.

Clinical observation shows that laser refractive surgery increases HOAs, mainly spherical and coma[1–5] (Llorente L, et al. IOVS 2002; 43:ARVO E-Abstract 2006). In particular, spherical aberrations induced by a procedure show a clear tendency that positive spherical aberration is induced after myopic treatment and a strong correlation with the amount of attempted dioptric power correction in myopic and hyperopic treatments. Spherical aberration is not only 1 of the most important HOAs that degrade retinal image quality; it also affects the subjective refraction of defocus because of the interaction between defocus and spherical aberration.[6] In other words, adding an appropriate amount of defocus when spherical aberration exists can make retinal image quality better than the same amount of spherical aberration with zero defocus. Therefore, if a significant amount of spherical aberration is uncorrected or induced after a surgical procedure, the full correction of defocus may not be the best way to obtain the best surgical outcomes.

Several studies propose possible reasons for induced spherical aberrations as well as algorithms to correct them. Holladay and coauthors[7] report that corneal asphericity increases after laser in situ keratomileusis (LASIK) for myopia, causing a functional vision decrease. Jímenez and coauthors[8] developed a theoret-

ical equation that represents the change in corneal asphericity. Gatinel and coauthors[9,10] also theoretically predicted corneal asphericity changes after myopic and hyperopic laser refractive surgery. In a recent study, Anera et al.[11] made similar conclusions and found that a greater increase in corneal asphericity and subsequent decrease in visual performance were observed with higher degrees of myopia.

Changes in corneal asphericity can explain some of the induced spherical aberration because when the radius of curvature of a cornea is constant, corneal asphericity is a predominant factor affecting the amount of the aberration. The corneal wound-healing process could be another reason laser ablation induces HOAs. Huang and coauthors[12] developed a mathematical model of corneal surface smoothing. They mathematically modeled epithelial thickness modulations to explain regression and induction of the aberrations clinically observed after laser ablation. Porter et al.[13] recently found that in LASIK, the laser ablation, not the microkeratome cut, seems to be a bigger factor in inducing spherical aberration. However, there was wide variation in the responses of other Zernike modes across patients after the flap was cut.

Mrochen and Seiler[14] propose that the ablation depth per laser pulse across the cornea varies under the influence of a difference in the effective illumination area and reflection losses that occur during laser–tissue interaction. Jímenez and coauthors[15] theoretically investigated the effect of laser-ablation algorithms of reflection losses and the non-normal incidence of laser pulse on the anterior cornea. Dupps and Roberts[16] and Roberts[17,18] propose another mechanism for induced spherical aberration after surgery; that is, corneal shape or curvature change caused by the biomechanical response of the cornea.

Some studies propose modified ablation algorithms to compensate for the spherical aberration. Schwiegerling and Snyder[19] developed the ideal ablation pattern to correct the introduced spherical aberration based on clinical data after photorefractive keratectomy. Manns and coauthors[20] calculated the corneal asphericity of a postoperative cornea that produces zero primary spherical aberration.

More precise understanding of the sources of induced spherical aberrations is needed for more effective correction of lower-order aberrations and

HOAs. However, there is little evidence on how laser refractive surgery induces spherical aberrations. In this paper, we hypothesize that 2 factors induce spherical aberration: (1) the variable laser ablation depth per pulse at different locations on the cornea that is caused by the oblique incidence of the laser spot and (2) the corneal shape change caused by the biological response of the cornea. We use the term *biological response* to represent factors that may occur during and after laser refractive surgery. The factors could include the biomechanical and wound-healing responses of the cornea and unexpected corneal surface change caused by imperfect laser ablation. A theoretical eye model based on clinical observations was developed. The model takes into account the effects described above. We sought to separate the effect of each factor on induced spherical aberration. We also demonstrated that our model can quantitatively predict the change in corneal asphericity.

Patients and Methods

The aberration data were collected at the Refractive Surgery Center, University of Rochester, under protocol approved by the University of Rochester Research Subject Review Board. All patients signed an informed consent before they participated in the study.

Preoperative and postoperative spherical aberrations were measured with a Shack-Hartmann wavefront sensor (Zywave, Bausch & Lomb) in 32 myopic and 17 hyperopic eyes. Corneal asphericity in the same eyes was measured with an Orbscan II corneal topographer (Bausch & Lomb). All postoperative measurements were done 1 month after laser refractive surgery. The magnitude of spherical aberration for a 6.0 mm pupil was expressed in microns as the Zernike coefficient corresponding to spherical aberration (Z_4^0). All eyes had conventional LASIK with a Technolas 217 laser (Bausch & Lomb). The nomogram and ablation profile design were not adjusted preoperatively. Changes in the measured spherical aberration and asphericity between preoperative and postoperative values were compared with the theoretical prediction on the basis of the aspheric cornea model. The attempted correction of spherical refractive error ranged from $+5.19$ diopters (D) to -6.48 D.

Model of the Spherical Cornea

The cornea can be expressed as a rotationally symmetric surface with different radii of curvature and asphericities (conic constant or shape factor). A rotationally symmetric surface, $C(x)$, can be mathematically defined by the following equation:

$$C(x) = \frac{cx^2}{1 + \sqrt{1 - (1 + k)c^2 x^2}} \qquad (1)$$

where x is the radial distance from the cornea's center, k is asphericity, and c is the reciprocal of the corneal radius of curvature. A surface with $k > 0$, $k = 0$, and $-1 < k < 0$ represents an oblate spheroid, sphere, and prolate spheroid, respectively. This equation was used to define the preoperative aspheric cornea. In the calculation of spherical aberration induced by laser ablation, a conic constant of -0.3 and a radius of curvature of 7.8 mm were assumed as preoperative corneal parameters. These values were chosen as an average, although a wide range of radii of curvature and asphericity of the normal cornea has been reported.

To obtain the postoperative cornea, an ablation thickness profile was calculated with the spherical Munnerlyn algorithm.[21] The effect of the oblique incidence of the laser spot across the cornea on the ablation depth was taken into account when the ablation profile was computed. The equations proposed by Mrochen and Seiler[15] were used to calculate the loss of ablation depth per pulse caused by the non-normal incidence of the laser spot. This calculated ablation depth per pulse with the effect of oblique incidence of the laser spot is referred to as the *variable ablation depth* in this paper. The postoperative cornea, $C_{postOP}(x)$, was simply defined by subtracting the ablation profile from the preoperative cornea as shown by

$$C_{postOP}(x) = C_{preOP}(x) - T_{ablation}(r) \qquad (2)$$

where $C_{preOP}(x)$ is a preoperative corneal profile calculated from the equation 1 and $T_{ablation}(x)$ is an ablation thickness profile based on the Munnerlyn algorithm.

Calculation of Spherical Aberration

Once the preoperative and postoperative corneal surfaces were calculated, a conventional ray-tracing program (CodeV, Optical Research Associates) was used to compute the spherical aberration generated by the preoperative and postoperative corneal surface profiles. With the same program, Zernike polynomials were fit to the ray-tracing results to compute the magnitude of Zernike spherical aberration (Z_4^0) for comparison with the clinically measured data. The sign convention of spherical aberration recommended by the VSIA Standards Taskforce team[22] was used. This simulation was conducted for a range of correction from -10.0 D (myopic treatment) to $+10.0$ D (hyperopic treatment) in 1.0 D steps. The asphericity of preoperative and postoperative corneas was also calculated to evaluate the effect of laser ablation on the change in corneal asphericity. All spherical aberration and corneal asphericity measurements and calculations were for a 6.0 mm pupil.
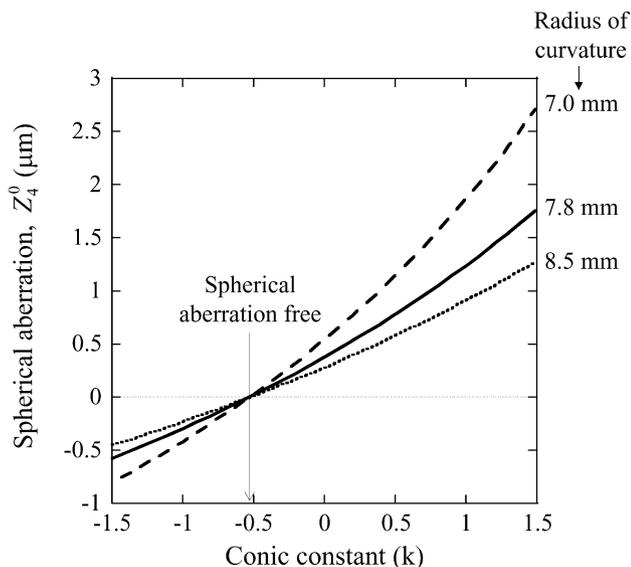
Results

Spherical Aberration of Rotationally Symmetric Cornea

Figure 1 shows the spherical aberration generated by rotationally symmetric corneal surfaces with different radii of curvature and asphericities. More positive spherical aberration is produced with a larger conic constant (more oblate spheroid). If the conic constant is larger than that of the spherical aberration-free cornea, a smaller radius of curvature (steeper cornea) would cause more positive spherical aberration. The conic constant in which the spherical aberration is zero is independent of the radius of curvature when the refractive index is constant. The conic constant for the spherical aberration-free cornea is approximately -0.53 when the refractive index of the cornea is assumed to be 1.376.

Spherical Aberration Induced by Refractive Surgery

Figure 2 summarizes clinical observations of the change in spherical aberration after myopic and hyperopic LASIK. Change in the spherical aberration expressed as a Zernike coefficient, Z_4^0, is the difference between preoperative and postoperative spherical aber-

ration; that is, postoperative spherical aberration – preoperative spherical aberration. In myopic treatment, positive spherical aberration increased. However, negative spherical aberration increased after hyperopic treatment. In both procedures, there was a significant correlation between the induced spherical aberration and the amount of the attempted defocus correction. Separate regression analysis of the myopic data and the hyperopic data yielded a correlation coefficient (r) of 66% and 64%, respectively. Based on these data, the correlation between the change in spherical aberration and the attempted defocus correction can be described by the following linear equations:

$$\Delta SA_{myopic} = -0.0465 \times D - 0.0096 \quad \text{in myopic correction} \quad (3)$$

and

$$\Delta SA_{hyperopic} = -0.0952 \times D - 0.1961 \quad \text{in hyperopic correction} \quad (4)$$

where ΔSA is the induced spherical aberration and D is the attempted defocus correction in diopters. Corresponding regression functions of equations 3 and 4 are represented by solid gray lines in Figure 2.

From the slopes of equations 3 and 4, with the same amount of defocus correction, the magnitude of the induced spherical aberration by a hyperopic procedure is larger than that induced by a myopic procedure by a factor of approximately 2.

Effect of Oblique Incidence of Laser Spot

A conventional algorithm that has been used to calculate an ablation profile in laser refractive surgery is based on the Munnerlyn equation that assumes a constant ablation depth of each laser pulse over the entire cornea. Recent studies, however, propose the ablation depth is variable, mainly due to the oblique incidence of laser pulse on the cornea. Because the corneal surface is curved, the efficiency of laser ablation decreases as each pulse hits the cornea farther from the center. Maximum ablation efficiency can be achieved when the laser pulse hits the corneal surface with a normal incidence angle. Figure 3 shows the calculated spherical aberration induced by conventional refractive surgery with fixed and variable ablation depths. An induced spherical aberration with a fixed

Figure 1. Theoretical calculation of spherical aberration produced by a rotationally symmetric cornea with different radii of curvature (7.0 mm, 7.8 mm, and 8.5 mm) and asphericities (conic constant), k, ranged from −1.5 to +1.5. Spherical aberration is zero when corneal asphericity, k, equals −0.53 when the refractive index of the cornea is 1.376.

ablation depth is shown by the dashed line. In both the myopic and hyperopic groups, the theoretical expectation with the fixed ablation depth has a tendency to be opposite that of the clinical data, represented by solid circles. Theoretically, more negative and positive spherical aberrations are induced in myopic corrections and hyperopic corrections, respectively.
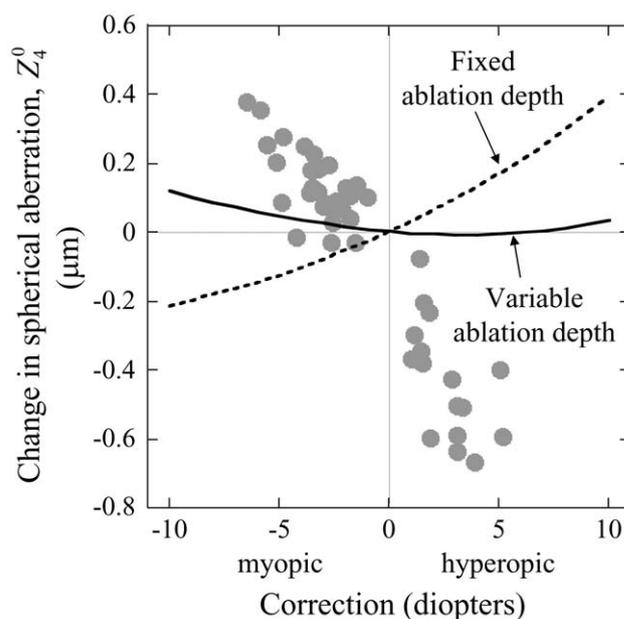
However, with the variable ablation depth (solid line in Figure 3) caused by the oblique incidence of the laser spot, there is qualitative agreement with the clinical data. Positive spherical aberration in myopic correction tends to increase with a larger amount of defocus correction. Almost no spherical aberration in hyperopic correction is induced. However, a significant quantitative discrepancy between the theory and clinical data remains, although the overall tendency of the theoretical prediction seems to better fit the clinical data than with a fixed ablation depth.

Effect of Biological Response of the Cornea

A hypothesis that could account for this remaining discrepancy is the biological response of the cornea. In myopic treatments, corneal biomechanics cause the central cornea to flatten and the peripheral cornea to steepen. The corneal epithelium after refractive surgery tends to fill in the abruptly changed surface to maintain a smooth surface profile. This corneal wound-healing response is included in biological factors for hypothesis. In simulation, the biological response of the cornea in terms of the amount of flattening and steepening required to account for the observed induced spherical aberration was quantitatively modeled. Figure 4 shows a biological model used to calculate the theoretical effect of the biological corneal surface change on the induced spherical aberration. In myopic treatment (Figure 4, *top*), the optical zone is divided into flattening and steepening zones. The flattening zone diameter is assumed to correspond to a central area that is 1.0 mm smaller than the optical zone diameter. Therefore, the steepening zone is an outer annular area with a width of 0.5 mm. In hyperopic treatment (Figure 4, *bottom*), the steepening and flattening zones are defined as a central area and an outer annular area, respectively. The magnitude of the biological effect, M_{bio}, is defined as a percentage of the amount of defocus correction in diopters. The actual
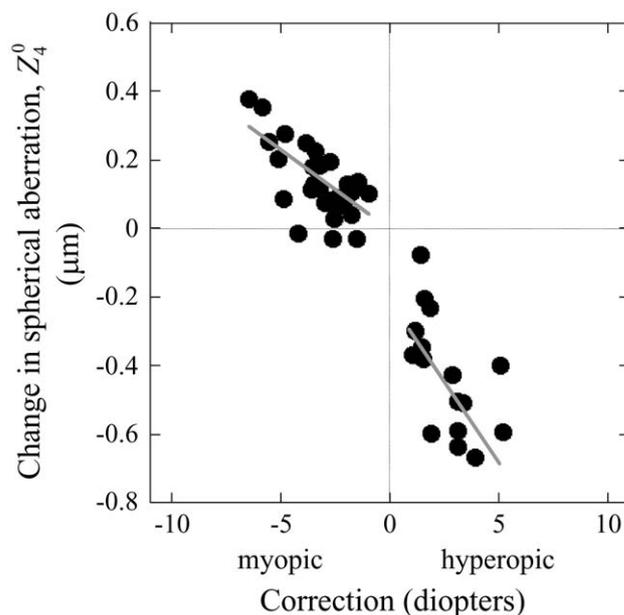
Figure 2. Clinically observed change in spherical aberration in myopic and hyperopic corrections expressed as a Zernike coefficient (Z_4^0) in microns. The change was computed by subtracting the measured preoperative spherical aberration from the postoperative one. The gray lines represent the best-fit linear regression performed on myopic and hyperopic data separately.

Figure 3. Theoretical expectations of the induced spherical aberration when assuming the fixed ablation depth per pulse (dashed line) and the variable ablation depth (solid line) due to oblique incidence of laser pulse across the cornea. The clinically observed data of the induced spherical aberration (filled circles) in Figure 2 is presented for comparison.

change in dioptric power in the flattening and steepening zones of the cornea can be described by

$$P_{\text{steep}} = M_{\text{bio}} \times |D| \qquad (5)$$

$$P_{\text{flat}} = -M_{\text{bio}} \times |D| \qquad (6)$$

where P is the dioptric power change in each zone caused by the biological response of the cornea and $|D|$ is the magnitude of defocus correction in diopters. It was assumed that the magnitude of the dioptric power change is identical in flattening and steepening zones. The minus sign in equation 6 indicates surface flattening. The dioptric power change in each flattening and steeping zone of the postoperative cornea caused by the biological response was taken into account, as was the effect of the variable ablation depth. In simulation, the magnitude M_{bio} was adjusted until the calculated spherical aberration provided the best fit to the clinical data.

Figure 5 shows the result of the theoretical prediction (solid line) of the induced spherical aberration when the effects of both the variable ablation depth and the biological corneal surface change are taken into account. For comparison, the clinical data represented by the gray circles are superimposed. In myopic correction, the magnitude of the corneal biological response for the best fit to the clinical data was 7% of the amount of defocus correction in diopters. Central flattening and peripheral steepening occurred. However, different trends for the biological corneal surface change in a hyperopic correction were found. The magnitude of the hyperopic biological effect was 25%, 3 times larger than that of the myopic correction. Moreover, in hyperopic correction, the direction of the biological response was opposite that of myopic correction; that is, central steepening and peripheral flattening were required to obtain the best fit to the clinically observed data.

Discussion

The eye model we present successfully explains the large difference in the induced spherical aberration between clinical data and the theory predicted from the original Munnerlyn algorithm. Each effect, the variable ablation depth and the biological response of the cornea, could account for approximately 50% of the discrepancy in the induced spherical aberration be-

tween clinical observation (filled circles) and theoretical prediction (dashed line) shown in Figure 3.

Changes in corneal asphericity after laser ablation could account for some of the induced spherical
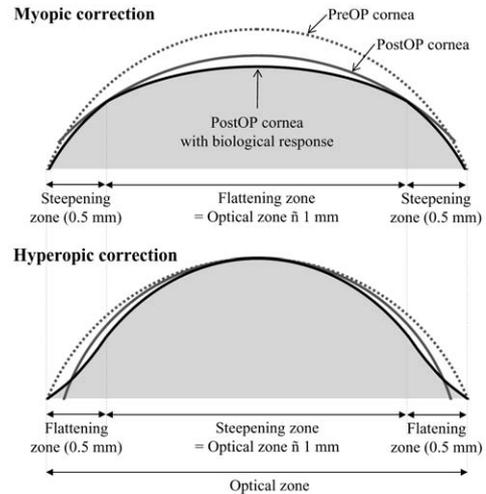
Figure 4. Schematic diagram of a model of the biological response of the cornea to explain the induced spherical aberration after myopic (*top*) and hyperopic (*bottom*) treatment. The dotted line indicates the preoperative cornea. The black and gray solid lines represent the postoperative corneas with and without the biological effect, respectively. Flattening and steepening zones in both procedures were also defined by millimeters in diameter.
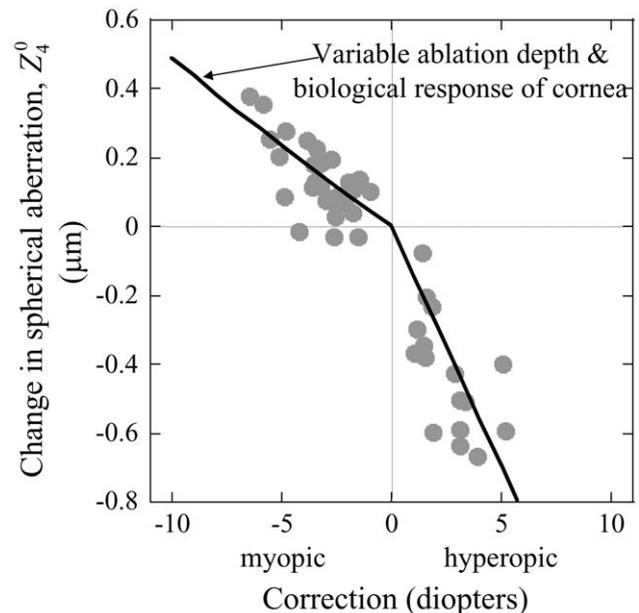
Figure 5. Comparison of the clinical data of the induced spherical aberration (filled circles) with theoretical expectations taking into account effects of the variable ablation depth and the biological response of the cornea (solid line).
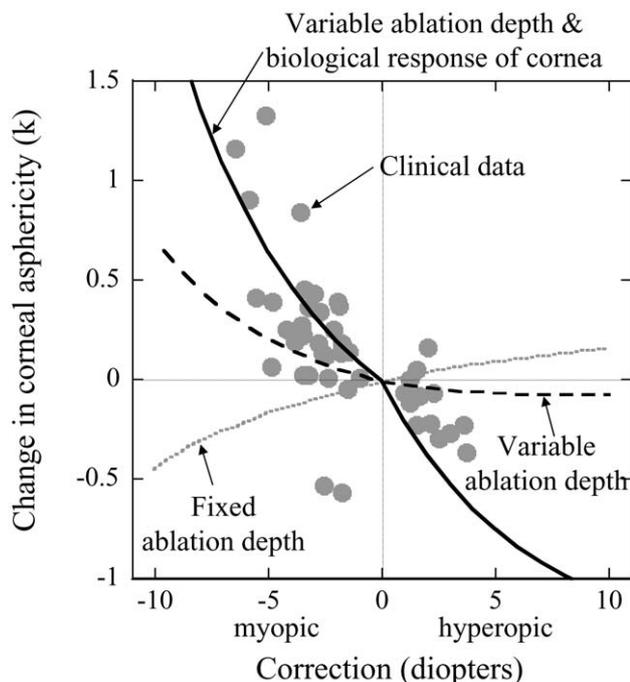
Figure 6. The clinically measured change in corneal asphericity (solid circles). For comparison, theoretical predictions from the model were also shown for 3 different conditions: a fixed ablation depth (gray dotted line), a variable ablation depth only (dashed line), and the biological response of the cornea in addition to the variable ablation depth (solid line).
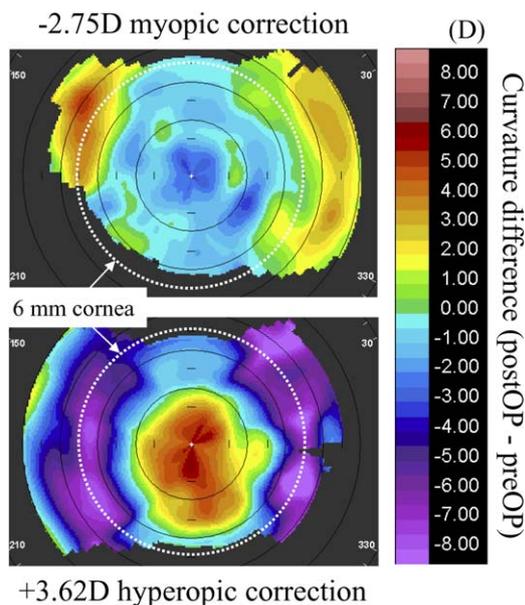
Figure 7. Tangential curvature difference maps of eyes that had myopic (*top*) and hyperopic (*bottom*) corrections. The difference maps were generated by subtracting the preoperative curvature map from the postoperative curvature map. The smallest solid black ring represents a 3.0 mm cornea in diameter, and there is a 2.0 mm difference in diameter between each ring. The dashed white circles represent the boundary of a 6.0 mm optical zone.

aberration. Our spherical cornea model was tested to evaluate a change in corneal asphericity with the same conditions used to calculate the induced spherical aberration. Figure 6 shows the measured and calculated changes in corneal asphericity after myopic and hyperopic procedures. Our clinical data (solid gray circles) show a similar trend in the spherical aberration change. As earlier studies report, corneal asphericity increased after a myopic procedure. In contrast, a hyperopic procedure caused a decrease in corneal asphericity. Predictions from our model with different conditions were also shown with curves in Figure 6. When the fixed ablation depth is assumed (gray dotted line), corneal asphericity predicted with the theory tends to change toward a direction opposite to the data. By adding the effect of the variable ablation depth to the model (dashed line) only, a qualitative tendency follows the clinical data even though the quantitative discrepancy is still large. With the effects of both the variable ablation depth and the biological response of the cornea (solid line), there is good agreement between the prediction and the clinical observations. We also found that the variability in the corneal asphericity clinical data is larger than that in spherical aberration, as shown by the gray circles in Figures 6 and 5, respectively. The discrepancy between the clinical data and the theoretical prediction is also larger in corneal asphericity than in spherical aberration. This may indicate that spherical aberration is a better predictor than corneal asphericity when estimating the optical quality of a postoperative cornea.

To further evaluate our biological cornea model, Orbscan corneal topography was taken before and after myopic and hyperopic procedures. Figure 7 shows tangential curvature difference maps obtained by subtracting the preoperative map from the postoperative map of the myopic and hyperopic groups. Figure 7, *top*, and Figure 7, *bottom*, represent myopic and hyperopic corrections, respectively, with a 6.0 mm optical zone. Because a myopic correction is supposed to generate a flatter cornea, a negative power distribution (blue–green) smaller than about 5.0 mm diameter (the second black ring from the center) can be seen in the central cornea. However, the negative power gradually changes to positive power (red) as the corneal diameter becomes larger than 5.0 mm. Positive power can be observed along the dotted circle representing the

6.0 mm optical zone size (white dashed ring), indicating that peripheral steepening occurs after laser ablation. In the eye with hyperopic correction, peripheral flattening (negative power distribution in the map [blue–purple]) that starts from approximately 3.0 mm in diameter is observed along the same optical zone boundary. For a 6.0 mm diameter cornea, the corneal topography clearly shows what is expected from the biological model. The postoperative cornea surface outside about the 6.0 mm diameter becomes steeper again, as an early study proposed.[18] This indicates that in hyperopic correction, there may be multiple zones of corneal curvature change, midperipheral flattening, and peripheral steepening. This may be because an ablation profile for hyperopic correction has 2 transition zones in the midperiphery and periphery. We also found that by comparing the magnitudes of power change along a 6.0 mm zone, the hyperopic procedure caused approximately 3.8 times larger power changes than myopic correction. With the difference in the amount of defocus correction, this is similar to what we predicted in our biological cornea model for induced spherical aberration; that is, the magnitude of the hyperopic biological response is larger than the response to myopic correction by a factor of 3. MacRae[23] made a similar prediction, noting that there were 3 "transition points" in each hemimeridian with hyperopic correction and hyperopic ablation and only 1 with myopic correction. This limits the amount of hyperopia correctable with hyperopic ablation to one third that seen clinically with myopia.

All companies developing a laser system for refractive surgery build in empirical adjustments in the ablation profiles designs. Typically, these are defocus undercorrection for myopic treatment and defocus overcorrection for hyperopic treatment. It is important to discuss how actual ablation profiles obtained from these adjustments affect our results because in our calculation, the adjustments were not considered, although the clinical data included them. If the adjustments were made based on rescaling a surgeon's attempted correction in terms of spherical dioptric power and no other special adjustment was made to intentionally correct the induced spherical aberration, it simply affects the level of contribution of biological response of the cornea to the induced spherical aberration.

In figures showing the clinical data, the x-axis (attempted correction in diopters) must be rescaled so that the range is smaller for myopic correction due to the built-in undercorrection and larger for hyperopic correction due to the built-in overcorrection. The scaling change makes slopes of best-fit equations steeper for myopic correction and flatter for hyperopic correction. This change in slopes of those equations indicates that the difference in magnitude of the cornea's biological response between myopic and hyperopic treatments is not as large as the factor of 3 that we found in the current model with no adjustment. In terms of the induced spherical aberration after laser refractive surgery, the empirical adjustments in dioptric defocus correction do not affect directions of the biological response of the cornea in myopic and hyperopic treatment hypothesized in our model. It results in an increase in the contribution of the cornea's biological response to the induced spherical aberration in myopic correction and a decrease in hyperopic correction. In other words, central steepening and peripheral flattening are still required in hyperopic treatment to explain the clinically observed spherical aberration induced by laser refractive surgery. We confirmed this by calculating the induced spherical aberration with the actual magnitude of the correction used by the laser ablation algorithm. However, central flattening and peripheral steepening for hyperopic correction by Roberts[18] biomechanical and Huang and coauthors'[12] epithelial smoothing models have been proposed to explain the clinically observed defocus changes. It would be interesting to see in a future study whether our biological model can explain some of the clinical observations in defocus changes and hyperopic shifts after myopic and hyperopic corrections.

Although our hypothesis of the biological response of the cornea explained the clinical data of the induced spherical aberration and the corneal surface change, it was hard to separate each biomechanical and healing response of the cornea. It is essential to understand precisely how each effect occurs and contributes to the HOAs induced by laser refractive surgery. Assuming the biomechanical response can occur earlier than the wound-healing response encourages us to develop a more robust way to measure corneal surface changes immediately after, or even during, laser refractive surgery.

In conclusion, an eye model that takes into account the effects of ablation efficiency and the biological response of the cornea was shown to effectively explain how refractive surgery induces spherical aberration. Further investigations, such as studies of individual variability in the magnitude of corneal biomechanics, and a better understanding of corneal wound-healing responses are needed for more complete knowledge of surgically induced HOAs to approach true aberration-free laser ablation. This model can be incorporated into an ablation algorithm to compensate for induced amounts of spherical aberration, improving the outcome of conventional and customized refractive surgery.

References

1. Oliver KM, Hemenger RP, Corbett MC, et al. Corneal optical aberrations induced by photorefractive keratectomy. J Refract Surg 1997; 13:246–254
2. Miller JM, Anwaruddin R, Straub J, Schwiegerling J. Higher order aberrations in normal, dilated, intraocular lens, and laser in situ keratomileusis corneas. J Refract Surg 2002; 18:S579–S583
3. Mrochen M, Kaemmerer M, Mierdel P, Seiler T. Increased higher-order optical aberrations after laser refractive surgery; a problem of subclinical decentration. J Cataract Refract Surg 2001; 27:362–369
4. Moreno-Barriuso E, Merayo Lloves J, Marcos S, et al. Ocular aberrations before and after myopic corneal refractive surgery: LASIK-induced changes measured with laser ray tracing. Invest Ophthalmol Vis Sci 2001; 42:1396–1403
5. Oshika T, Klyce SD, Applegate RA, et al. Comparison of corneal wavefront aberrations after photorefractive keratectomy and laser in situ keratomileusis. Am J Ophthalmol 1999; 127:1–7
6. Applegate RA, Marsack JD, Ramos R, Sarver EJ. Interaction between aberrations to improve or reduce visual performance. J Cataract Refract Surg 2003; 29:1487–1495
7. Holladay JT, Dudeja DR, Chang J. Functional vision and corneal changes after laser in situ keratomileusis determined by contrast sensitivity, glare testing, and corneal topography. J Cataract Refract Surg 1999; 25:663–669
8. Jímenez JR, Anera RG, Jímenez del Barco L. Equation for corneal asphericity after corneal refractive surgery. J Refract Surg 2003; 19:65–69
9. Gatinel D, Hoang-Xuan T, Azar DT. Determination of corneal asphericity after myopia surgery with the excimer laser: a mathematical model. Invest Ophthalmol Vis Sci 2001; 42:1736–1742
10. Gatinel D, Malet J, Hoang-Xuan T, Azar DT. Corneal asphericity change after excimer laser hyperopic surgery: theoretical effects on corneal profiles and corresponding Zernike expansions. Invest Ophthalmol Vis Sci 2004; 45:1349–1359
11. Anera RG, Jímenez JR, Jímenez del Barco L, et al. Changes in corneal asphericity after laser in situ keratomileusis. J Cataract Refract Surg 2003; 29:762–768
12. Huang D, Tang ML, Shekhar R. Mathematical model of corneal surface smoothing after laser refractive surgery. Am J Ophthalmol 2003; 135:267–278
13. Porter J, MacRae S, Yoon G, et al. Separate effects of the microkeratome incision and laser ablation on the eye's wave aberration. Am J Ophthalmol 2003; 136: 327–337
14. Mrochen M, Seiler T. Influence of corneal curvature on calculation of ablation patterns used in photorefractive laser surgery. J Refract Surg 2001; 17:S584–S587
15. Jímenez JR, Anera RG, del Barco LJ, Hita E. Effect on laser-ablation algorithms of reflection losses and nonnormal incidence on the anterior cornea. Appl Phys Letters 2002; 81:1521–1523
16. Dupps WJ Jr, Roberts C. Effect of acute biomechanical changes on corneal curvature after photokeratectomy. J Refract Surg 2001; 17:658–669
17. Roberts C. The cornea is not a piece of plastic [editorial]. J Refract Surg 2000; 16:407–413
18. Roberts C. Biomechanics of the cornea and wavefront-guided laser refractive surgery. J Refract Surg 2002; 18: S589–S592
19. Schwiegerling J, Snyder RW. Corneal ablation patterns to correct for spherical aberration in photorefractive keratectomy. J Cataract Refract Surg 2000; 26:214–221
20. Manns F, Ho A, Parel J-M, Culbertson W. Ablation profiles for wavefront-guided correction of myopia and primary spherical aberration. J Cataract Refract Surg 2002; 28:766–774
21. Munnerlyn CR, Koons SJ, Marshall J. Photorefractive keratectomy: a technique for laser refractive surgery. J Cataract Refract Surg 1988; 14:46–52
22. Thibos LN, Applegate RA, Schwiegerling JT, Webb R. Standards for reporting the optical aberrations of eyes. VSIA Standards Taskforce Members. OSA Trends in Optics and Photonics 2000; 35:232–244
23. MacRae S. Excimer ablation design and elliptical transition zones. J Cataract Refract Surg 1999; 25:1191–1197